DOI: 10.11817/j.ysxb.1004.0609.2021-42082

胶莱盆地郭城－崖子断裂带金矿集区剥蚀程度及深部找矿潜力

陈原林[1,2]，李　欢[1,2]，郑朝阳[3]，李大兜[4]

(1. 中南大学 地球科学与信息物理学院，长沙 410083；
2. 中南大学 有色金属成矿预测与地质环境监测教育部重点实验室，长沙 410083；
3. 贵州大学 资源与环境工程学院，贵阳 550025；
4. 山东省第一地质矿产勘查院，济南 250100)

摘　要：胶莱盆地郭城－崖子断裂带是国内近年来发现的一个重要金成矿区，陆续探明了一批大中型–超大型金矿床。然而，该矿集区的深部找矿勘查工作一直没有取得重大突破。本文通过系统采集成矿岩体样品，挑选磷灰石单颗粒矿物，采用裂变径迹热年代学方法，揭示研究区岩体(矿体)温度–时间演化关系，反演岩体(矿体)热演化历史，解析成矿后构造对矿床的改造，定量计算岩体(矿体)抬升–剥蚀速率，总结矿床变化保存规律。结果表明：郭城－崖子断裂带金矿集区主要经历了110~20 Ma和20~0 Ma两个阶段的成矿后热史，两阶段不均匀的隆升冷却过程受到了太平洋多期增生扩张过程的影响。根据对磷灰石裂变径迹热历史演化分析，结合区域古地温梯度、成矿深度以及侏罗纪和白垩纪陆相沉积地层厚度，计算得出研究区内白垩纪至今地层总剥蚀深度约为5.33 km，金矿带矿体成矿深度为5.62 km，表明郭城－崖子断裂带内矿体遭受了较大程度的抬升剥蚀，推测断裂带南西向地层剥蚀少的部位有较大的找矿潜力，并建立了郭城－崖子断裂带深部金矿体定位模型，评价了深部找矿潜力。

关键词：鹊山岩体；牧牛山岩体；热史模拟；隆升剥蚀；深部勘查；成矿深度

文章编号：1004-0609(2022)-09-2819-16　　**中图分类号**：P597.3；P618.51　　**文献标志码**：A

引文格式：陈原林, 李　欢, 郑朝阳, 等. 胶莱盆地郭城－崖子断裂带金矿集区剥蚀程度及深部找矿潜力[J]. 中国有色金属学报, 2022, 32(9): 2819−2834. DOI: 10.11817/j.ysxb.1004.0609.2021-42082

CHEN Yuan-lin, LI Huan, ZHENG Chao-yang, et al. Denudation degree and deep prospecting potential of gold deposits in Guocheng-Yazi fault zone, Jiaolai basin[J]. The Chinese Journal of Nonferrous Metals, 2022, 32(9): 2819−2834. DOI: 10.11817/j.ysxb.1004.0609.2021-42082

胶莱盆地郭城－崖子断裂带是胶东金成矿域的重要组成部分，区内分布有大量的金矿床(见图1)。该区域处于华北板块与苏鲁－大别造山带的交接部位，区内构造复杂，岩浆活动强烈，发育了以鹊山岩体、牧牛山岩体以及大量中生代中基性脉岩[1−2]，也发育了一系列大中小型金矿床(点)，如蓬家夼、宋家沟(发云夼)、龙口－土堆、辽上、西涝口、西井口、东井口、南地口、马石店、前垂柳、东北缘等，累计查明资源储量150t以上[3−4]。前人对部分金矿(点)的成矿地质特征、成矿时代、成矿过程、

基金项目：国家重点研发计划资助项目(2016YFC0600104)；中国黄金集团公司–山东烟台鑫泰黄金矿业有限责任公司地质科研项目(XY-DZ2020081)

收稿日期：2021-07-15；**修订日期**：2021-10-08

通信作者：李　欢，教授，博士；电话：18827415616；E-mail：lihuan@csu.edu.cn

动力学背景、成矿物质来源、成矿流体性质、金矿床的成矿过程和元素共生分异机制，开展了大量研究并取得诸多重要进展[5−21]。然而，由于郭城－崖子断裂带深部勘探和研究程度较低，该区域隆升剥蚀过程和深部找矿潜力一直不清楚，严重制约了后续深部找矿勘查工作的部署。胶莱盆地郭城－崖子断裂带内已知的金矿体均直接产于牧牛山岩体、荆山群大理岩及莱阳群砾岩[3−4]。区域构造隆升和剥蚀作用，直接控制和影响矿床形成及之后的保存与变化过程[22−24]。前人针对胶东西北部地区花岗岩开展了系统的磷灰石裂变径迹热年代学研究，结果显示岩体自~110 Ma 以来的平均剥蚀速率为(0.0303±0.0044) mm/a，属于慢速剥露的范畴，这对矿床的保存非常有利。根据该剥蚀速率计算，该地区白垩纪以来的剥蚀量仅为2.0~4.2 km，远未达到金矿最大成矿深度，显示该地区深部金矿找矿潜力巨大[25]。对胶西北地区玲珑金矿田和焦家金矿田开展了锆石(U-Th)/He的测试工作，用以研究这两个矿田隆升剥蚀程度的研究。测试结果表明：玲珑矿田锆石(U-Th)/He 年龄主要为80~100 Ma，焦家矿田锆石(U-Th)/He 年龄主要为90~105 Ma；根据年龄−高程关系估算，该地区隆升速率大致与全球造山带型金矿剥露速率相当(大约60 m/Ma)，而玲珑矿田总体比焦家矿田成矿后多剥露了600~900 m；焦家矿田应该具有比玲珑矿田更大的深部找矿潜力[26−27]。这些研究工作表明，低温热年代学对找矿工作的开展与部署具有一定的指导与启示作用，且磷灰石裂变径迹热年代学可以对矿床形成以后的变化与保存过程提供直观、定量的示踪和评价[25, 28−33]。低温热年代学对矿床的变化保存以及成矿后热历史演化等方面的研究，在胶东金矿集区取得了较为理想的成果[27, 34−40]。因此，在进一步总结前人的研究成果的基础上，结合低温热年代学技术，调整找矿思路，厘清控矿要素，建立成矿系列，对矿床的保存变化进行定量评估，无疑是寻找深部隐伏矿体，进军“第二找矿空间”并取得新的找矿突破的必由之路。本文首次通过对胶莱盆地郭城－崖子断裂带金矿集区内不同标高牧牛山岩体、鹊山岩体的磷灰石进行裂变径迹热年代学研究，以期定量查明矿床成矿后经历的隆升与剥蚀作用，为该区域成矿与深部找矿勘查工作提供新的理论借鉴。

1 地质背景

研究区位于胶东金矿集区东部，牟平－乳山成矿带中南部，受牟平－即墨断裂带南端的NE向郭城断裂和崖子断裂控制；其东南为苏鲁超高压变质带，西南临胶莱盆地，西北为胶北地体(见图1)。研究区处于不同地质构造单元交汇部位，地质构造复杂，不同期次的各种定向构造交织叠加在一起，多期构造活动相互错动、改造和继承，呈现出各期构造发育程度悬殊的展布格局。区域内出露地层比较简单，发育有新太古代胶东岩群，岩性主要为斜长角闪岩、黑云变粒岩和黑云斜长片麻岩，呈NW向带状分布在桃村断裂以西；古元古代荆山群，岩性主要为大理岩和变粒岩，主要分布于郭城断裂的下盘；中生代莱阳群、青山群及王氏群，为一套陆相碎屑沉积岩，岩性以砾岩、砂岩和粉砂岩为主，在区域内广泛分布；新生代第四系，岩性为砂、砾石、砂质亚黏土，主要分布于区域内较大河流的河床中[41]。区内断裂构造十分发育。断裂产状及发育程度明显受控于牟平－即墨断裂带，走向以NE向为主(NE 40°~50°)，断裂的规模较大，断裂带宽6~100 m，其自西向东，分布有桃村断裂、郭城断裂和崖子断裂；其次发育有NNE向、EW向和NW向断裂。研究区内断裂构造具有多期活化特征，随形成时代更新，断裂由EW向、NE向、NNE向、NW向、EW向逆时针旋转，且具有不同断裂部位发育程度不同的特点[41]。区域岩浆活动频繁，广泛发育有基性、中性和酸性岩浆岩。其中以酸性岩为主，大面积出露牧牛山岩体(二长花岗岩)，岩体内发育有大量荆山群变粒岩、大理岩包体。此外，燕山期各类脉岩密集发育，脉岩走向在NE 40°~50°之间，倾向NW，倾角大都在60°~80°之间(见图2)。

胶莱盆地郭城－崖子断裂带金矿集区位于中生代莱阳群砾岩与古元古代荆山群变质岩接触带附近，发育一系列低角度层间滑动断层，控制了区域蚀变角砾岩型金矿床的产出。前人研究表明：郭城－崖子断裂带金矿床与胶东其他类型金矿是同一构造背景、同一成因、同一时代形成的、产于不同构造部位、不同围岩条件下的不同自然类型矿床(见图2)[11−17, 42]。伴随着中生代的幔隆作用，岩石圈减薄，胶东地区大规模花岗岩侵位形成热隆−伸展

构造，为成矿提供了有利空间；白垩纪大规模岩浆作用、流体活动、伸展拆离是中生代盆地边缘区金矿成矿的关键因素[43−46]。龙口－土堆金矿床金矿化的赋矿岩石以黄铁绢英岩、荆山群大理岩和牧牛山岩体二长花岗岩为主。胶莱盆地郭城－崖子断裂带鹊山岩体－牧牛山岩体野外地质特征如图3所示。

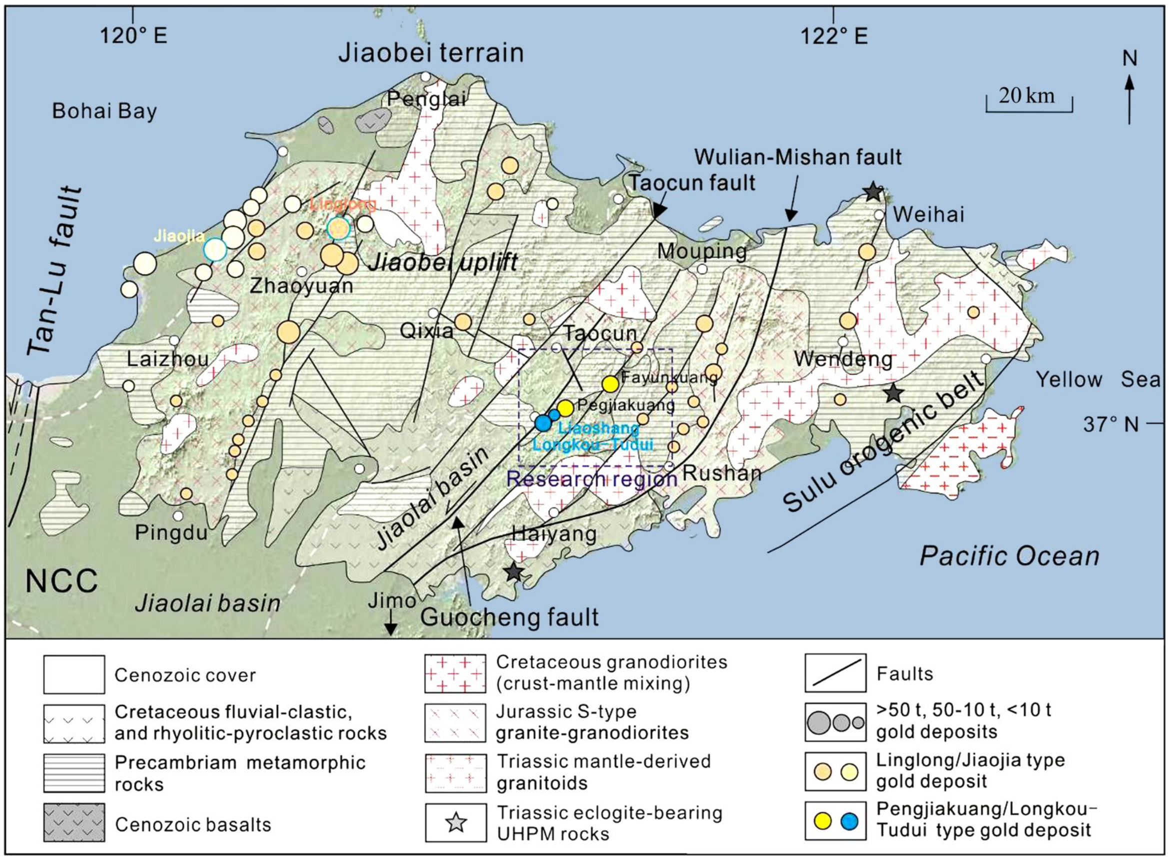

图1　胶东区域地质图(据文献[17]修改)

Fig. 1　Regional geological map of Jiaodong (modified from Ref.[17])

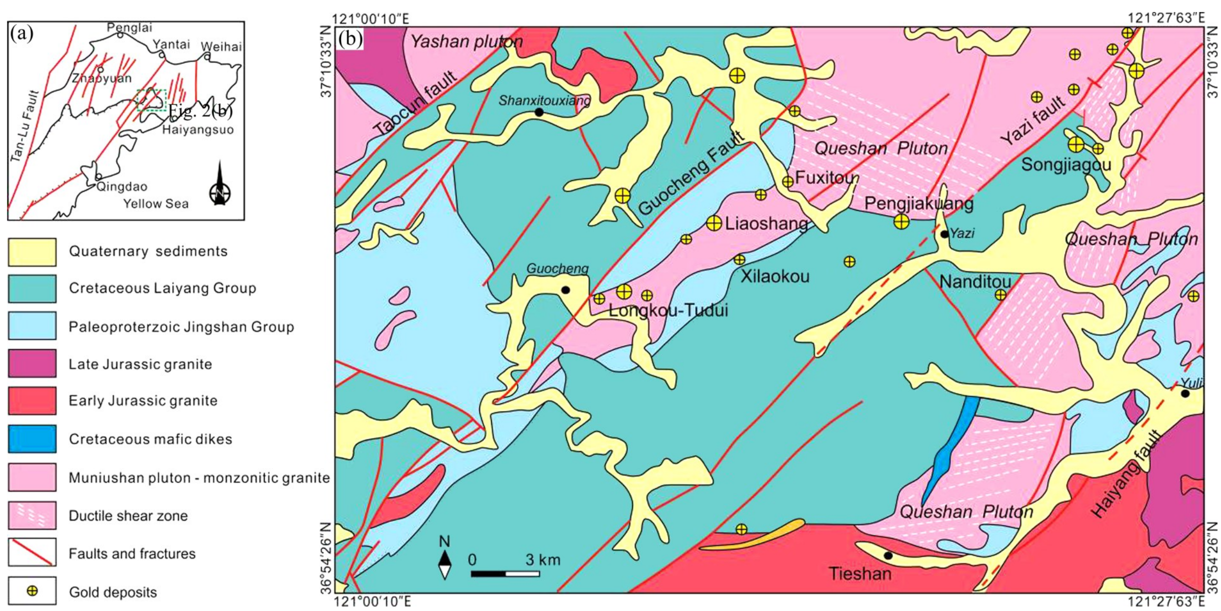

图2　胶莱盆地东北缘郭城–崖子断裂带区域地质图(据文献[41]修改)

Fig. 2　Regional geological map of ore concentration area of Guocheng-Yazi fault in northeast margin of Jiaolai Basin (modified from Ref. [41])

矿体受断层、断裂模式控制，现控制标高从地表(海拔约+200 m)至−1500 m开采或勘探。矿体呈透镜体和细脉的形式，矿体与围岩之间的接触不平整且无明显界线。单个矿脉的长度为100~1000 m，宽度为0.5~11 m，向下延伸50~300 m。大多走向NNE和NEE，倾角15°~25°(局部可达35°)NW倾或40°~60°SE倾，部分矿体NW向或EW向。矿化优先富集在构造缓倾斜或弯曲处，产状由陡变缓。这些部位具有高度的膨胀性和渗透性，为热液流体聚集和金属矿沉淀提供了空间[17]。通过对研究区隆升和冷却历史的恢复，对比分析研究区内金矿自形成后至今的变化保存过程，可以对区内金矿的深部潜力做出预测，进而为深部找矿勘探工作提供关键性指示信息。

2 样品测试方法和结果

本次采用地表不同标高和钻孔深部岩心横穿矿区法进行样品采集，共采集了7件样品进行磷灰石裂变径迹测试，采样位置及高程使用高精度GPS标定(见表1)。样品岩性主要为鹊山岩体的糜棱花岗岩、以及牧牛山岩体的二长花岗岩。磷灰石裂变径迹测试在北京泽康恩科技有限公司裂变径迹实验室进行，实验步骤见文献[33]。裂变径迹年龄根据IUGS推荐的Zeta(ζ)常数法和标准裂变径迹年龄方程计算[47]。

对每个样品挑选磷灰石，同时进行裂变径迹分析，获得裂变径迹年龄及平均径迹长度，测试结果及分布特征见表2、图4。$P(\chi^2)$值是判断所测单颗粒磷灰石裂变径迹年龄是否属于同组年龄的概率参数[48]，通常以5%为界限；$P(\chi^2)$＞5%时表明径迹年龄属于同一年龄组，表明裂变径迹年龄受到相同热事件的影响；$P(\chi^2)$＜5%时表明径迹年龄是混合年龄，代表裂变径迹年龄受到不同期次热事件的影响[28−29, 33]。由表2可看出，各样品裂变径迹年龄值的$P(\chi^2)$均大于＞5%，说明对于每个样品而言，所测的磷灰石颗粒曾经历过相同或相似的地质热史过程。蚀刻半径D_{par}是与结晶c轴平行的裂变径迹蚀像的最大直径。对于长时间处于70 ℃以上温度条件的磷灰石颗粒而言，其裂变径迹年龄及长度与颗粒的溶蚀度密切相关[49−50]。D_{par}作为用来定量表征磷灰石溶解度的一个指标，可在显微镜下直接测定。通常D_{par}越小，径迹退火速率越快。通过测定D_{par}区分出不同动力学组分，使得样品内具有相似动力学行为的磷灰石颗粒的裂变径迹长度的差别反映所经历热史的差别。胶莱盆地郭城−崖子断裂带金矿集区蚀刻半径D_{par}为1.55~1.87，径迹退火速率稳定，表明所测试样品的地质热史过程差别较小。

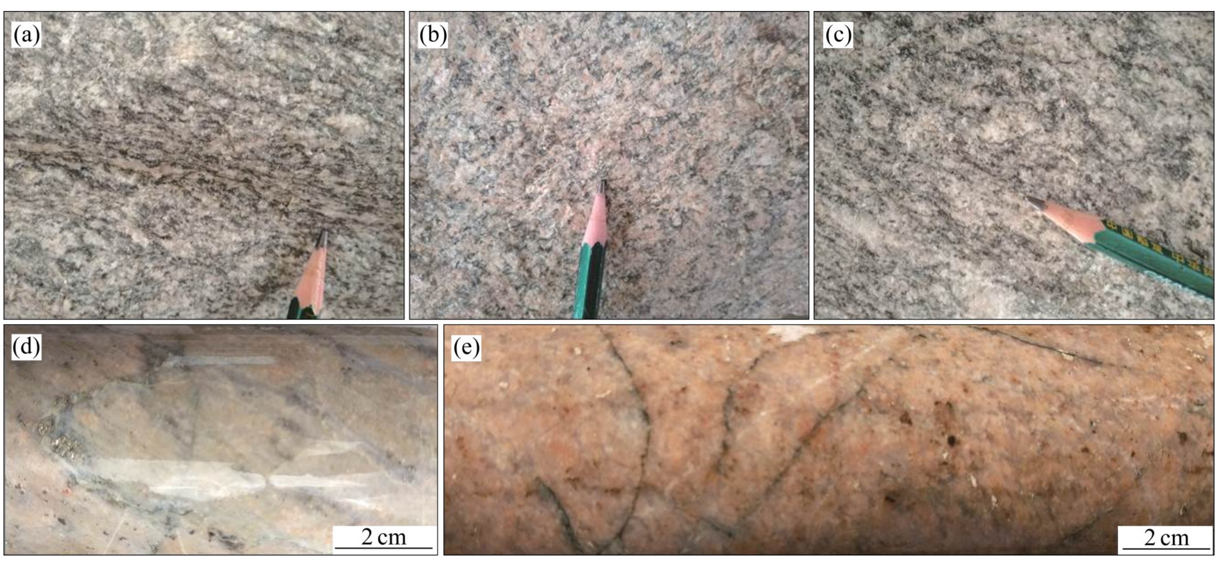

图3 胶莱盆地郭城−崖子断裂带鹊山岩体−牧牛山岩体野外地质特征

Fig.3 Geological characteristics of Queshan pluton-Muniushan pluton in Guocheng-Yazi fault zone in Jiaolai Basin: (a) Queshan pluton(Pengjiakuang); (b) Queshan pluton (Fayunkuang); (c) Queshan pluton(Songjiagou); (d) Muniushan pluton in core of TFZK2020-3 borehole; (e) Muniushan pluton in core of ZK2019-2 borehole

表 1　胶莱盆地郭城—崖子断裂带金矿集区采样位置及样品描述

Table 1　Sampling location and Sample description of gold deposits area in Guocheng-Yazi fault zone in Jiaolai basin

Sample No.	Locality	Lithology	Elevation/m	Latitude	Longitude	Analysis
QS-1	North Songjiagou Road	Queshan pluton	+80	37°7′31.74″	121°23′10.71″	AFT
QS-2	Pengjiakuang North	Queshan pluton	+225	37°6′53.13″	121°15′16.02″	AFT
QS-3	Pengjiakuang North	Queshan pluton	+310	37°7′41.72″	121°16′57.78″	AFT
QS-4	Pengjiakuang North	Queshan pluton	+400	37°8′33.23″	121°18′05.45″	AFT
MUS-1	ZK2019-2(drilling depth 692 m)	Muniushan pluton	−500	37°4′07.45″	121°10′50.27″	AFT
MUS-2	ZK2019-2(drilling depth 1568 m)	Muniushan pluton	−1350	37°4′07.45″	121°10′50.27″	AFT
MUS-3	TFZK2020-3(drilling depth 1960 m)	Queshan pluton	−1770	37°4′08.00″	121°09′36.30″	AFT

表 2　胶莱盆地郭城—崖子断裂带金矿集区磷灰石裂变径迹分析结果表

Table 2　Apatite fission track analysis results of gold deposits in Guocheng-Yazi fault zone in Jiaolai basin

Sample No.	Grain, n	ρ_s/ (10^5·cm^{-2}) (Ns)	ρ_i/ (10^5·cm^{-2}) (Ni)	ρ_d/ (10^5·cm^{-2}) (N)	U/ 10^{-6}	$P(\chi^2)$/ %	Central age/Ma (±1σ)	Pooled age/Ma (±1σ)	L/ Mm (N)	D_{par}/ μm
MUS-1	3	1.654 (40)	14.97 (362)	16.028 (4841)	10.88	91.7	35±6	35±6	13.6±1.9 (8)	1.83
MUS-2	35	0.961 (160)	18.881 (3144)	15.811 (4841)	15.19	9.7	16±2	16±2	12.5±1.8 (117)	1.63
MUS-3	40	0.492 (134)	10.625 (2892)	12.332 (4841)	10.70	84.0	11±1	11±1	12.1±1.8 (44)	1.55
QS-1	35	2.328 (737)	20.681 (6546)	13.202 (4841)	19.99	63.4	29±2	29±2	13.1±1.8 (176)	1.87
QS-2	35	1.364 (385)	14.346 (4050)	14.072 (4841)	12.31	57.4	26±2	26±2	13.0±1.8 (136)	1.84
QS-3	35	1.471 (408)	13.59 (3770)	14.942 (4841)	10.66	31.5	32±2	32±2	12.8±1.9 (122)	1.73
QS-4	35	2.174 (600)	22.016 (6077)	15.811 (4841)	17.79	61.1	30±2	30±2	12.7±1.8 (129)	1.82

测试结果显示(见图4)，6件磷灰石样品的裂变径迹年龄均呈单峰状分布，大致分为三组年龄峰值，即：(11±1) Ma、(26±2) Ma和(35±6) Ma。

3　磷灰石热史模拟

3.1　热史模拟方法

成矿过程中热液活动产生的地质热事件超过磷灰石的封闭温度时，磷灰石内部的裂变径迹将逐渐消失进而发生退火行为；当温度下降至退火温度以下时，裂变径迹计时器打开[28−29]。因此，根据磷灰石的退火行为可以模拟出地质体最近一次经历的构造热史演化过程称为正演，利用磷灰石裂变径迹的实测数据进行热史反演，可以检验正演数据的可靠性。通过磷灰石的正演和反演模拟相结合，更能真实反映出地质体的热史信息[33, 51−55]。

根据本次所测试的磷灰石数据，借助HeFTY软件进行热史反演，模拟矿集区不同矿床从成矿至现今的热演化史。模拟的限定条件为：1) 设定磷灰石完全退火的约束条件为140 ℃，地表温度限定为20 ℃；2) 裂变径迹的模拟温度设定为20~300 ℃；3) 模拟的温度−时间曲线设定为10000 条；4) 将反

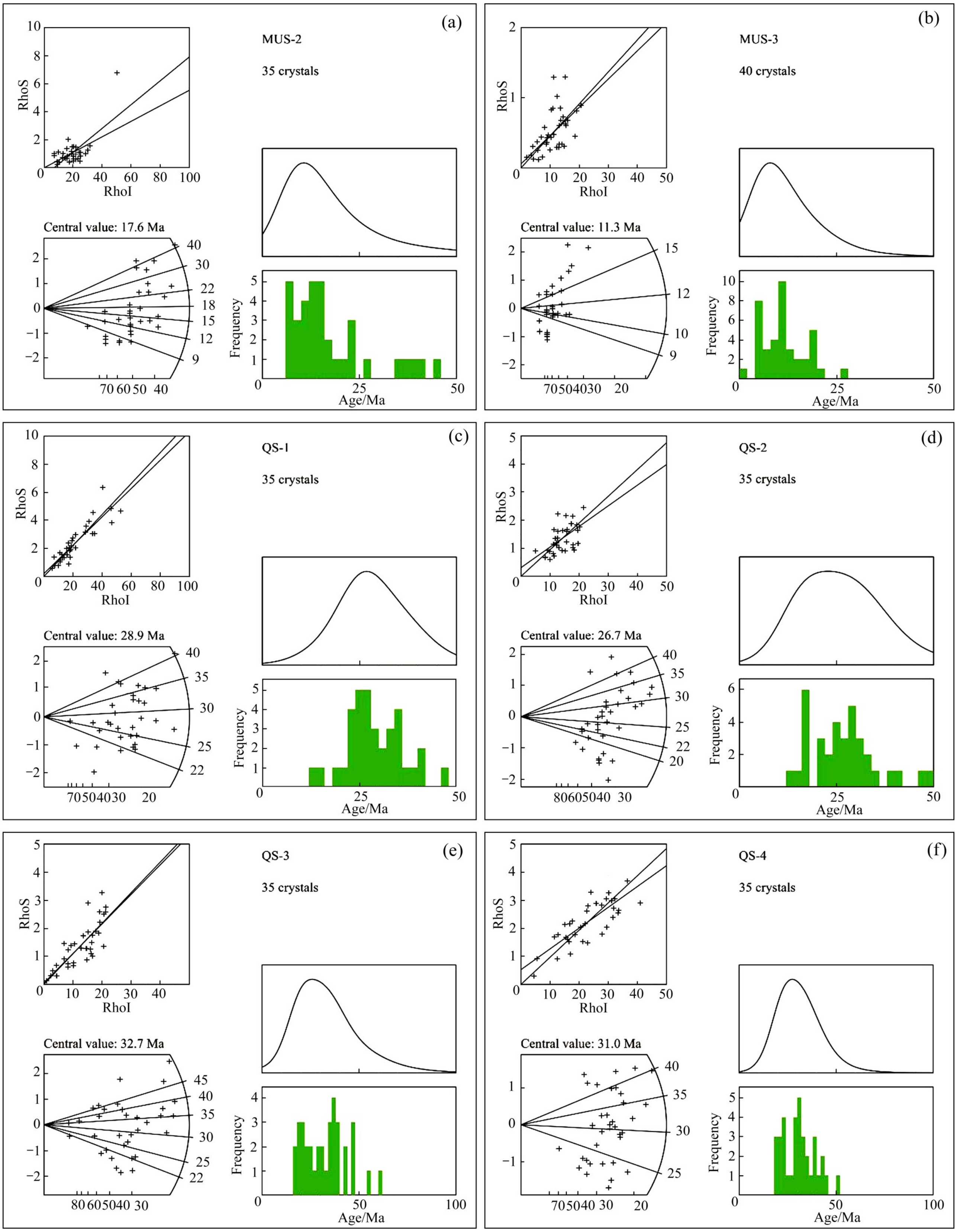

图 4　胶莱盆地郭城—崖子断裂带磷灰石单颗粒年龄分布直方图、频率曲线及单颗粒年龄雷达图

Fig. 4　Age distribution histograms, frequency curves and single particle age radar maps of apatite in Guocheng-Yazi fault zone in Jiaolai basin: (a) MUS-2; (b) MUS-3; (c) QS-1; (d) QS-2; (e) QS-3; (f) QS-4

演结果与实测数据进行比较，利用GOF值(拟合优度)来判断模拟年龄、径迹长度与观测值的吻合程度。模拟结果见图5和6。结果显示，反演的GOF值均大于0.5(见图6)，表明样品的正演和反演结果是可靠的，能够真实反映出郭城－崖子断裂带金矿集区经历的构造演化热史。

3.2　模拟结果分析

裂变径迹年龄通常反映的是其封闭温度对应的时限，不同的矿物具有不同的裂变径迹退火温度，一般认为磷灰石的退火温度为140 ℃。为了解矿区成矿热液的温度，税鹏[56](2019)研究了龙口－土堆主成矿期石英流体包裹体，推测成矿流体为中高盐度的H_2O-CO_2-NaCl-$CaCl_2$体系；石英包裹体校正后均一温度为180.6~530 ℃，成矿作用早期均一温度达500~540 ℃，成矿温度属中高温；成矿压力为9.013×10^5~1.401×10^6 Pa，相当于成矿深度为3~4 km。谭俊等[17](2015)对郭城金矿带早期捕集的流体包裹体进行了研究，测得最终校正均一温度在500~540 ℃之间，成矿期的包裹体均一温度在300~450 ℃之间；表明成矿热液的温度高于磷灰石的退火温度，低于锆石的退火温度。本研究区内的成矿活动能够使磷灰石的裂变径迹发生完全退火作用，证明选择磷灰石作裂变径迹热史模拟是可行的。另外，郭城－崖子断裂带金矿集区的宏观地质特征显示：矿区内早期形成的岩体矿化微弱，而晚阶段形成的岩石往往蚀变强烈矿化富集，且构造对金矿化并无直接控制影响。这些特征暗示着早期成岩的流体与成矿并无直接联系，金矿化主要是在晚阶段的成岩过程中或是成岩以后发生的。磷灰石由于独特的退火温度，其裂变径迹年龄通常反映的是成岩以后的热事件年龄，因此可以认为磷灰石裂变径迹年龄能够代表郭城－崖子断裂带金矿集区的成矿热时代。

在本次研究的7件磷灰石裂变径迹样品中，MUS-1样品未获得有效径迹长度值，不具备统计学研究意义，本次不参与研究；其余6件样品的径迹长度分布范围为7.425~17.82 μm，平均长度为

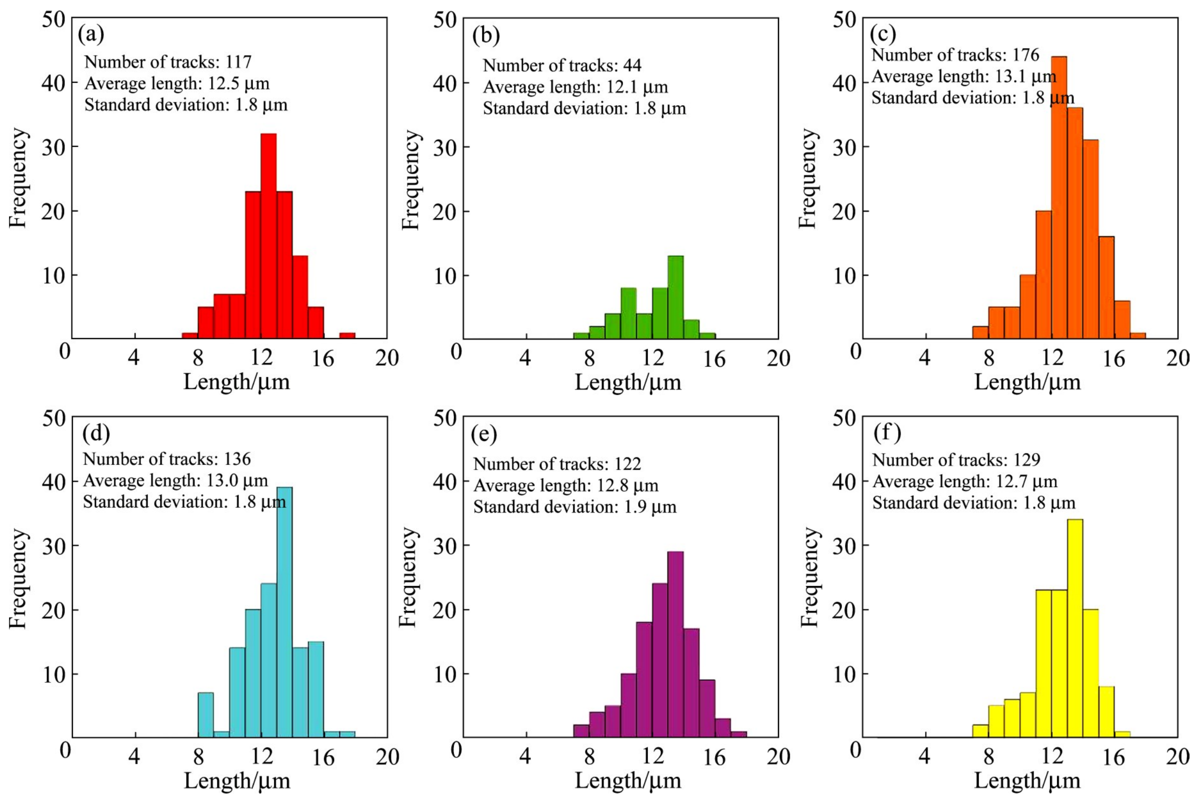

图5　胶莱盆地郭城－崖子断裂带金矿集区磷灰石裂变径迹长度分布图

Fig. 5　Distributions of apatite fission track length in gold deposit area of Guocheng-Yazi fault zone in Jiaolai basin: (a) MUS-2; (b) MUS-3; (c) QS-1; (d) QS-2; (e) QS-3; (f) QS-4

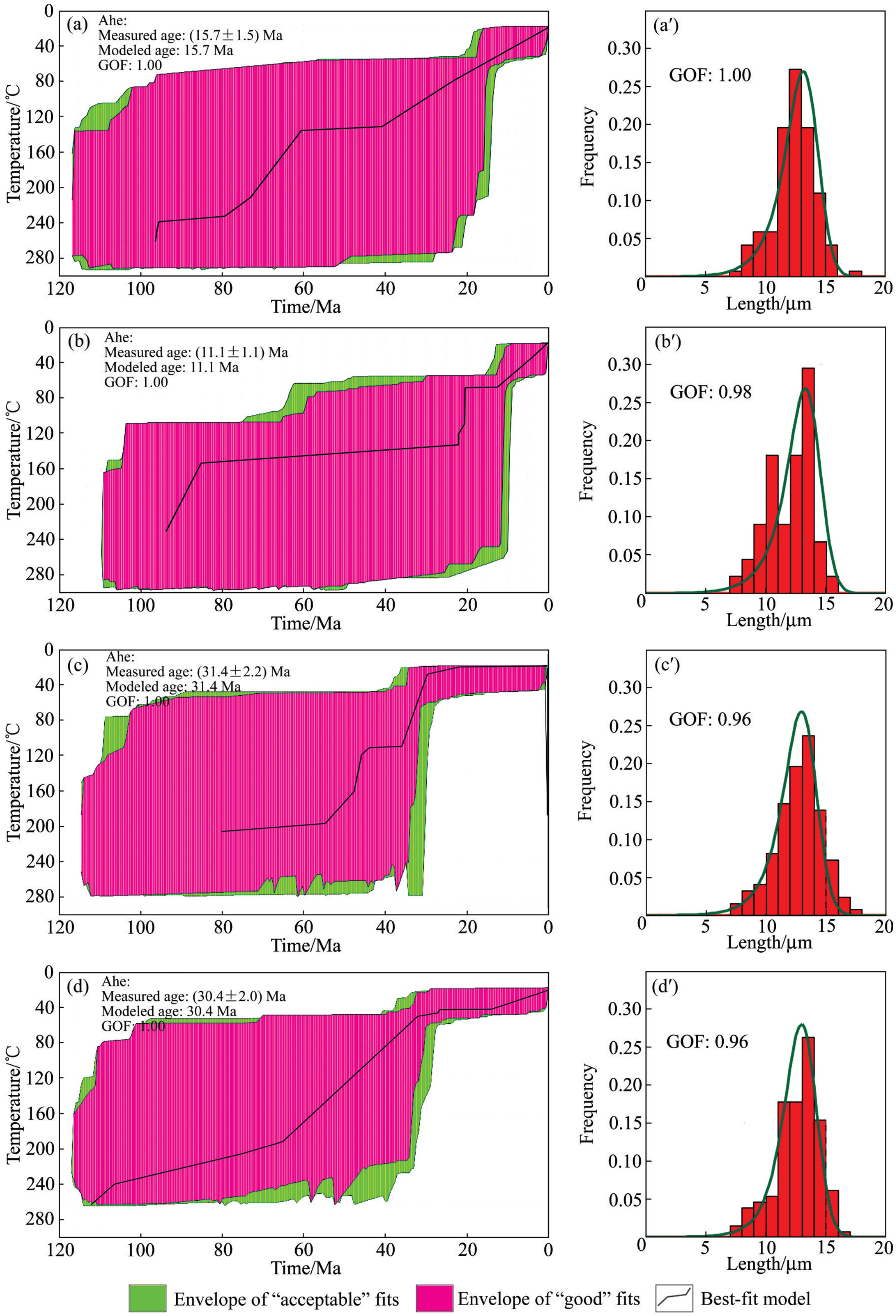

图 6 胶莱盆地郭城—崖子断裂带金矿集区磷灰石裂变径迹热史模拟结果

Fig. 6 Thermal history simulation results of apatite fission track in gold deposits area of Guocheng-Yazi fault zone in Jiaolai basin: (a), (a′) MUS-2; (b), (b′) MUS-3; (c), (c′) QS-3; (d), (d′) QS-4

(10.9±2.1) μm，峰值相对较宽，且均有一个峰值分布特征，在12~14 μm之间(见图5)。图6所示为胶莱盆地郭城−崖子断裂带金矿集区磷灰石裂变径迹热史模拟结果。从图6可知，样品峰值整体上较宽，表明样品中的部分径迹遭受了较长时间的退火作用。热史模拟结果显示，MUS-2、MUS-3、QS-3和QS-4等4件样品最佳模拟曲线高度相似(见图6)，指示所有样品均经历了相似的构造热演化过程。早白垩纪以来，牧牛山−鹊山岩体主要经历了两阶段构造抬升事件：第一期，早白垩世–中新世(约112~20 Ma)，样品均表现为快速降温状态，平均冷却速率约为2.2~3.3 ℃/Ma；第二期，中新世至今(约20~0 Ma)，样品均表现为缓慢降温状态，平均冷却速率约为0.9~2.5 ℃/Ma。资料显示，胶东地区古地温梯度为40 ℃/km，经计算可知，牧牛山−鹊山岩体在第一期快速冷却事件中的剥蚀量为4.04~5.37 km (平均值为4.62 km)，剥蚀速率为55~83 m/Ma(平均值为68 m/Ma)；其在第二期快速冷却事件中的剥蚀量为0.27~0.96 km(平均值为0.71 km)，剥蚀速率为23~63 m/Ma(平均值为43 m/Ma)，与区域上热年代学研究的结果基本相当[25−27, 57]。

4　讨论

4.1　区域性隆升剥蚀过程对比

胶莱盆地郭城−崖子断裂带的热历史演化对比研究表明(见图5和6)，蓬家夼金矿早于龙口−土堆金矿开始隆升剥蚀，金矿带发生差异化的隆升剥蚀事件；造成这一现象的原因可能是鹊山岩体自南西向北东俯冲于牧牛山岩体之下，致使上覆地层荆山群大理岩发生大规模的逆冲推覆，因而更靠近蓬家夼−龙口弧形构造带中心的蓬家夼金矿和辽上金矿先于稍远的龙口−土堆金矿隆升剥蚀。隆升过程中，拆离断层将断层两盘的岩石圈解耦，卸载和花岗岩在深部侵位的均衡效应使下盘上拱，非共轴变形使沿拆离断层连续发育花岗岩、糜棱岩化花岗岩、花岗质初糜棱岩和花岗质糜棱岩及伴生金矿床。断层上盘形态复杂，派生断裂和断陷盆地发育，并沉积了脆性变形控制的岩石序列(见图7)。

胶东大规模成矿作用发生在110~130 Ma[10, 20]，并且有130 Ma以前成矿作用的零星记录；成矿年龄的分布范围基本没有超出200~100 Ma，限定在侏罗纪和早白垩世。年代学资料证明，受胶莱盆地低角度断层控制的金矿形成时代为117~128 Ma。这与胶东北部金矿的形成时代115~126 Ma相同，从而表明它们是同一成矿期不同地质背景条件下的产物，同时有力地说明和验证了胶东地区在燕山晚期(120±10) Ma处于区域构造调整和转换、岩石圈强烈减薄的重要时期，也正是发生成矿大爆发的有利时期。全球洋底磁条带的研究[58]显示，太平洋自晚白垩世以来存在四个增生期, 从老到新对应的年代依次为97 Ma、58 Ma、36 Ma、10 Ma。牧牛山−鹊山岩体的磷灰石热年代学模拟结果显示，自晚白垩世以来，牧牛山−鹊山岩体经历了不均匀的隆升剥蚀过程，但总体处于不断隆升状态，这可能

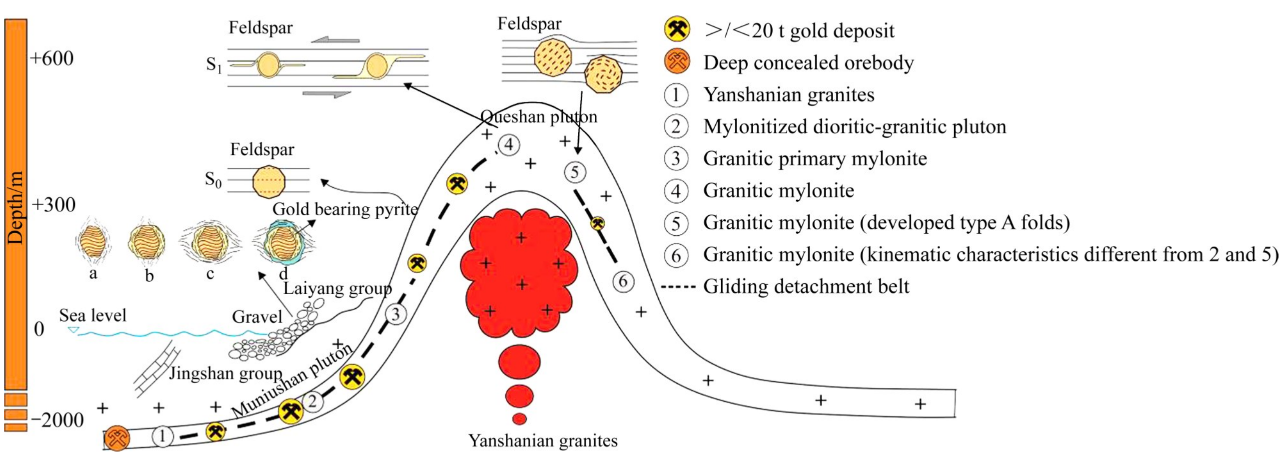

图7　基于鹊山岩体−牧牛山岩体磷灰石裂变径迹下的矿体隆升−剥蚀模式

Fig. 7　Ore body uplift-denudation model based on apatite fission track of Queshan pluton-Muniushan pluton

为太平洋洋底地壳不断增生的结果。

4.2 成矿后剥蚀程度及深部找矿潜力

郭城—崖子断裂带金矿集区主要产在荆山群大理岩、牧牛山岩体二长花岗岩和鹊山岩体内，是与岩浆侵入作用关系密切，其形成深度主要取决于岩浆的侵位深度，而岩浆的侵位深度决定了矿床形成深度的下限。定量估算成岩、成矿深度的方法主要有矿物平衡地质压力计法、流体包裹体压力计和构造校正测算法等[59−62]。

流体包裹体能够提供热液演化的温压信息是矿化压力的主要信息载体，运用流体包裹体压力计可以定量估算出矿床的成矿深度[62]。本文利用等容线相交法[60]进行估算，求得蓬家夼流体包裹体的捕获压力值为63~93 MPa。据 SIBSON 等[61](1998)断裂带内流体压力和深度之间进行分段拟合得到的两者间的非线性关系式，计算出蓬家夼金矿床的成矿深度为6.39~7.93 km，属于中成深度。宋家沟金矿包裹体的捕获压力值为40~62 MPa。成矿深度为5.01~6.34 km。龙口—土堆金矿流体包裹体的捕获压力为81~94 MPa，成矿深度为7.39~7.98 km。根据 ROEDDER[59](1979)利用 $NaCl$-H_2O 体系 P-T-D 图解进行成矿压力估算，辽上金矿白云石中的流体包裹体被捕获时，其压力值范围为12.16~27.22 MPa，成矿深度为1.22~2.72 km。总的来看，辽上金矿的成矿流体具有中等盐度、低密度的特征，成矿温度属中偏低温范围，成矿压力及深度为浅成范围。辽上金矿的成矿深度及温度、压力条件均较蓬家夼金矿、宋家沟金矿、龙口—土堆金矿小得多。通过计算可知，郭城—崖子断裂带金矿集区的成矿深度为1.22~7.93 km，平均为5.62 km。通过定量计算获得郭城—崖子断裂带金矿集区的成矿深度(见表3)，结合成矿环境特征及其经历的隆升作用时限进行分析，结果显示郭城—崖子断裂带金矿集区龙口—土堆金矿在成矿以后经历的剥蚀程度较低，其最大剥

表3 胶莱盆地郭城—崖子断裂带金矿集区矿床成矿地质环境特征

Table 3 Characteristics of metallogenic environment of gold deposit in Guocheng-Yazi Fault Zone, Jiaolai Basin

Typical deposits	Ore bearing geological units	Ore-controlling structure	Orebody scale	Main ore-forming phase	Metallogenic depth/km
Pengjiakuang	Laiyang Group, Jingshan Group	Pengjiakuang interlayer detachment fault zone near EW direction	Strike length 74−480 m, oblique depth 100−400 m, thickness 1.01−3.26 m, average 2.04 m	Gold-quartz-pyrite stage	6.39−7.93
Songjiagou	Laiyang Group	Upper plate steeply dipping fault and fracture-intensive zone of basin margin detachment structure	Monomer size is small, length is 10 m to dozens of meters, thickness is generally less than 2 m, control slant depth 40−200 m		5.01−6.34
Liaoshang	Jingshan Group and Muniushan pluton-monzonitic granite	NE-trending basin margin detachment structure	Ore body length 80−550 m, main ore body thickness 6.25 −16.79 m, single engineering ore body thickness maximum 47.00 m	Gold-pyrite-carbonate stage	1.22−2.72
Longkou-Tudui	Jingshan Group and Muniushan pluton-monzonitic granite	Slow dip structure of secondary fault in footwall of Guocheng fault	Length ranging from 10 m to tens of meters, thickness 0.8−3 m, slope depth 10−180 m, maximum slope depth 295 m	Gold-quartz-pyrite (carbonation) stage	7.39−7.98

蚀量远小于矿床的成矿深度。且目前探矿工程揭露表明，矿区的含矿岩体(牧牛山岩体二长花岗岩)未遭受大规模的断层破坏，证明龙口－土堆金矿床是一个保存较为完整的且与岩浆有关热液型金矿床，其深部及外围均具有良好的找矿潜力。

4.3　郭城－崖子断裂带金矿集区的找矿方向

根据对磷灰石裂变径迹热历史的演化分析，结合研究区古地温梯度、成矿深度以及侏罗纪和白垩纪陆相沉积地层厚度，计算得出研究区内白垩纪至今地层总剥蚀深度约为5.33 km，表明郭城－崖子断裂带内矿体遭受了一定程度的剥蚀。郭城－崖子断裂带内金矿带东北部地层剥蚀量大且埋深浅，而南西部地层剥蚀量相对较少，矿体的保存条件相对较好，找矿潜力较大。从已探明储量可知，辽上金矿的矿体相对西井口金矿的矿体保存得更好，主要因为辽上金矿处于构造交汇处，保存条件较好，而蓬家夼金矿处于EW向断裂浅部，保存条件较差。西涝口金矿、前垂柳金矿的地段可能找矿潜力更好。在龙口－土堆金矿区郭城断裂带，探明矿体主要分布在断裂带的下盘，而上盘矿体分布不明；上覆的莱阳群地层保护了下部的矿体，推测靠近断裂带且上覆莱阳群地层的区域有较大的找矿潜力(见图8)。

5　结论

1) 磷灰石裂变径迹热史模拟显示，郭城－崖子断裂带主要经历了110~20 Ma和20~0 Ma两个阶段的成矿后热史，两阶段不均匀的隆升冷却过程为太平洋洋底地壳多期增生的结果。

2) 结合热史模拟和深部验证钻孔揭露资料，构建了基于鹊山岩体－牧牛山岩体的磷灰石裂变径迹约束下的矿床隆升–剥蚀模式。

3) 根据对磷灰石裂变径迹热历史演化的分析，结合研究区古地温梯度、成矿深度以及侏罗纪和白垩纪陆相沉积地层厚度，计算得出研究区内白垩纪至今地层总剥蚀深度约为5.33 km，金矿带矿体的成矿深度为5.62 km，表明郭城－崖子断裂带内矿体遭受了较大程度的剥蚀，推测断裂带南西向地层剥蚀少的部位有较大的找矿潜力。

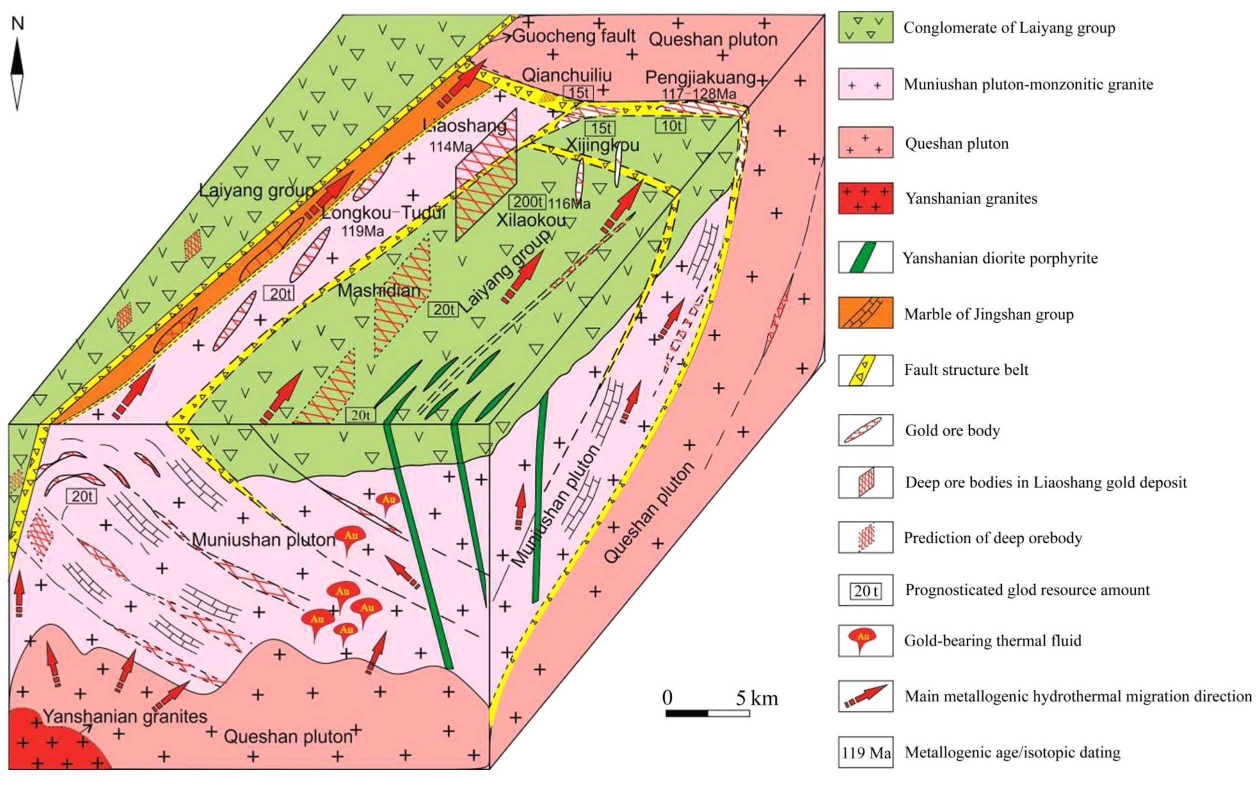

图8　胶莱盆地郭城－崖子断裂带金矿集区深部矿体定位模型

Fig. 8　Positioning model of deep ore bodies in gold deposits of Guocheng-Yazi fault zone in Jiaolai basin

致谢：

山东烟台鑫泰黄金矿业有限责任公司地质资源部高级工程师秦连元在野外采集样品工作中给予的帮助，中国地质大学(北京)袁万明教授在裂变径迹测试工作中给予的帮助，成文过程中得到了中国地质大学(武汉)孙华山老师、中南大学郑涵老师和吴经华博士的帮助和悉心指导，在此一并深表感谢！

REFERENCES

[1] 冯 波, 李红梅, 魏兴亮, 等. 胶东郭城地区牧牛山岩体年代学研究及其地质意义[J]. 黄金, 2013, 34(4): 24−28.
FENG Bo, LI Hong-mei, WEI Xing-liang, et al. Chronological study on Muniushan pluton in Guocheng District of Jiaodong Peninsula and its geological significance[J]. Gold, 2013, 34(4): 24−28.

[2] 夏增明, 刘俊来, 倪金龙, 等. 胶东东部鹊山变质核杂岩结构、演化及区域构造意义[J]. 中国科学: 地球科学, 2016, 46(3): 356−373.
XIA Zeng-ming, LIU Jun-lai, NI Jing-long, et al. Structure, evolution and regional tectonic implications of the Queshan metamorphic core complex in eastern Jiaodong Peninsula of China[J]. Science China Earth Sciences, 2016, 46(3): 356−373.

[3] 刘必政, 张继林, 冯 波, 等. 胶东郭城地区龙口: 土堆金矿区深部成矿潜力及找矿方向[J]. 黄金, 2019, 40(10): 10−13.
LIU Bi-zheng, ZHANG Ji-lin, FENG Bo, et al. Metallogenic potential and prospecting indications in the deep levels of Longkou-Tudui Gold District, Guocheng Area, Jiaodong[J]. Gold, 2019, 40(10): 10−13.

[4] 段留安, 魏有峰, 陈雄军, 等. 山东胶莱盆地东北缘前垂柳矿区金矿资源潜力分析[J]. 黄金科学技术, 2020, 28(5): 701−711.
DUAN Liu-an, WEI You-feng, CHEN Xiong-jun, et al. Potential evaluation of Qianchuiliu gold mineral resources in northeast margin of Jiaolai basin, Shandong Province[J]. Gold Science and Technology, 2020, 28(5): 701−711.

[5] 刘玉强, 史 辉, 李 军, 等. 胶莱盆地周边金矿床地质−地球物理−地球化学特征及找矿意义[J]. 地球学报, 2004, 25(6): 593−600.
LIU Yu-qiang, SHI Hui, LI Jun, et al. Geological, geophysical and geochemical characteristics of gold deposits around Jiaolai Basin, Shandong Province and their prospecting significance[J]. Acta Geoscientica Sinica, 2004, 25(6): 593−600.

[6] 刘玉强, 杨东来, 黄太岭, 等. 山东胶莱盆地金矿床地质特征及找矿方向[J]. 矿床地质, 1999, 18(3): 195−207.
LIU Yu-qiang, YANG Dong-lai, HUANG Tai-ling, et al. Geological characteristics and ore-prospecting targets in gold deposits of Jiaolai Basin, Shandong Province[J]. Mineral Deposits, 1999, 18(3): 195−207.

[7] 杨金中, 沈远超, 刘铁兵, 等. 山东蓬家夼金矿床成矿流体地球化学特征[J]. 矿床地质, 2000, 19(3): 235−244.
YANG Jing-zhong, SHEN Yuan-chao, LIU Tie-bing, et al. Geochemiical characteristics of ore-forming fluids in the Pengjiakuang gold deposit, Shandong Province[J]. Mineral Deposits, 2000, 19(3): 235−244.

[8] 张连昌, 沈远超, 刘铁兵, 等. 山东胶莱盆地北缘金矿 Ar-Ar 法和 Rb-Sr 等时线年龄与成矿时代[J]. 中国科学(D 辑), 2002, 32(9): 727−734.
ZHANG Lian-chang, SHEN Yuan-chao, LIU Tie-bing, et al. Ar-Ar and Rb-Sr isochron dating of the gold deposits on northern margin of the Jiaolai basin, Shandong, China[J]. Science in China(Series D), 2002, 32(9): 727−734.

[9] 李红梅, 魏俊浩, 王 启, 等. 山东土堆−沙旺金矿床同位素组成特征及矿床成因讨论[J]. 地球学报, 2010, 31(6): 791−802.
LI Hong-mei, WEI Jun-hao, WANG Qi, et al. Isotopic composition features and ore-forming mechanism of the Tudui-Shawang gold deposit in Shandong Province[J]. Acta Geoscientica Sinica, 2010, 31(6): 791−802.

[10] 李 杰, 张丽鹏, 李聪颖, 等. 胶东郭城金矿床黄铁矿 Rb-Sr 等时线年龄[J]. 中国地质, 2020, 47(3): 894−895.
LI Jie, ZHANG Li-peng, LI Cong-ying, et al. Rb-Sr isochron age of the Guocheng gold deposit in the Jiaodong Peninsula, Shandong[J]. Geology in China, 2020, 47(3): 894−895.

[11] 李 勇, 丁正江, 薄军委, 等. 胶莱盆地东北缘地区成矿元素地球化学特征及成矿潜力分析[J]. 黄金, 2018, 39(8): 15−21.
LI Yong, DING Zheng-jiang, BO Jun-wei, et al. Geochemical characteristics of ore-forming elements and metallogenic potentiality in the gold mineralization area of northeast margin of Jiaolai Basin[J]. Gold, 2018, 39(8): 15−21.

[12] 谭 俊, 魏俊浩, 杨春福, 等. 胶东郭城地区脉岩类岩石地球化学特征及成岩构造背景[J]. 地质学报, 2006, 80(8): 1177−1188.
TAN Jun, WEI Jun-hao, YANG Chun-fu, et al. Geochemstry and tectonic setting of dikes in the Guocheng area, Jiaodong Peninsula[J]. Acta Geologica Sinica, 2006, 80(8): 1177−1188.

[13] TAN Jun, WEI Jun-hao, GUO Ling-li, et al. LA-ICP-MS zircon U-Pb dating and phenocryst EPMA of dikes, Guocheng, Jiaodong Peninsula: Implications for North China Craton lithosphere evolution[J]. Science in China Series D: Earth Sciences, 2008, 51(10): 1483−1500.

[14] TAN Jun, WEI Jun-hao, SHI Wen-jie, et al. Origin of dyke swarms by mixing of metasomatized subcontinental lithospheric mantle-derived and lower crustal magmas in the Guocheng fault belt, Jiaodong Peninsula, North China Craton[J]. Geological Journal, 2013, 48(5): 516−530.

[15] TAN Jun, WEI Jun-hao, AUDÉTAT A, et al. Source of metals in the Guocheng gold deposit, Jiaodong Peninsula, North China Craton: link to Early Cretaceous mafic magmatism originating from Paleoproterozoic metasomatized lithospheric mantle[J]. Ore Geology Reviews, 2012, 48: 70−87.

[16] TAN Jun, WEI Jun-hao, HE Huai-yu, et al. Noble gases in pyrites from the Guocheng-Liaoshang gold belt in the Jiaodong province: Evidence for a mantle source of gold[J]. Chemical Geology, 2018, 480: 105−115.

[17] TAN Jun, WEI Jun-hao, LI Yan-jun, et al. Origin and geodynamic significance of fault-hosted massive sulfide gold deposits from the Guocheng-Liaoshang metallogenic belt, eastern Jiaodong Peninsula: Rb-Sr dating, and H-O-S-Pb isotopic constraints[J]. Ore Geology Reviews, 2015, 65: 687−700.

[18] ZHANG Lian-chang, SHEN Yuan-chao, LIU Tie-bing, et al. $^{40}Ar/^{39}Ar$ and Rb-Sr isochron dating of the gold deposits on northern margin of the Jiaolai Basin, Shandong, China[J]. Science in China Series D: Earth Sciences, 2003, 46(7): 708−718.

[19] CHENG Shao-bo, LIU Zhen-jiang, WANG Qing-fei, et al. SHRIMP zircon U-Pb dating and Hf isotope analyses of the Muniushan Monzogranite, Guocheng, Jiaobei Terrane, China: Implications for the tectonic evolution of the Jiao-Liao-Ji Belt, North China Craton[J]. Precambrian Research, 2017, 301: 36−48.

[20] LI Jun-jian, ZHANG Peng-peng, LI Guo-hua, et al. Formation of the Liaoshang gold deposit, Jiaodong Peninsula, eastern China: Evidence from geochronology and geochemistry[J]. Geological Journal, 2020, 55(8): 5903−5913.

[21] LIU Xiao-yang, TAN Jun, HE Huai-yu, et al. Origin of the Tudui-Shawang gold deposit, Jiaodong Peninsula, North China Craton: Constraints from fluid inclusion and H-O-He-Ar-S-Pb isotopic compositions[J]. Ore Geology Reviews, 2021, 133: 104125.

[22] 彭省临, 樊俊昌, 邵拥军, 等. 矿山深部隐伏矿定位预测关键技术新突破[J]. 中国有色金属学报, 2012, 22(3): 844−853.

PENG Sheng-lin, FAN Jun-chang, SHAO Yong-jun, et al. New breakthrough in key technologies of location prediction about deep concealed ore bodies of mine[J]. The Chinese Journal of Nonferrous Metals, 2012, 22(3): 844−853.

[23] 杨 斌, 高星, 彭省临, 等. 招平断裂带大尹格庄−后仓段深部矿体定位预测[J]. 中国有色金属学报, 2012, 22(3): 872−879.

YANG Bin, GAO Xing, PENG Sheng-lin, et al. Oriental prognosis of deep orebodies in Dayingezhuang-Houcang mining area of Zhaoping fault zone[J]. The Chinese Journal of Nonferrous Metals, 2012, 22(3): 872−879.

[24] 邓 军, 杨立强, 葛良胜, 等. 滇西富碱斑岩型金成矿系统特征与变化保存[J]. 岩石学报, 2010, 26(6): 1633−1645.

DENG Jun, YANG Li-qiang, GE Liang-shen, et al. Character and post-ore changes, modifications and preservation of Cenozoic alkali-rich porphyry gold metallogenic system in western Yunnan, China[J]. Acta Petrologica Sinica, 2010, 26(6): 1633−1645.

[25] 柳振江, 王建平, 郑德文, 等. 胶东西北部金矿剥蚀程度及找矿潜力和方向——来自磷灰石裂变径迹热年代学的证据[J]. 岩石学报, 2010, 26(12): 3597−3611.

LIU Zhen-jiang, WANG Jian-ping, ZHENG De-wen, et al. Exploration prospect and post-ore denudation in the northwestern Jiaodong Gold Province, China: Evidence from apatite fission track thermochronology[J]. Acta Petrologica Sinica, 2010, 26(12): 3597−3611.

[26] 孙华山, 韩静波, 申玉科, 等. 胶西北玲珑、焦家金矿田锆石(U-Th)/He年龄及其对成矿后剥露程度的指示[J]. 地球科学, 2016, 41(4): 644−654.

SUN Hua-shan, HAN Jing-bo, SHEN Yu-ke, et al. Zircon (U-Th)/He age and its implication for post-mineralization exhumation degree of Linglong and Jiaojia goldfields, northwest Jiaodong, China[J]. Earth Science, 2016, 41(4): 644−654.

[27] SUN Hua-shan, LI Huan, LIU Liu, et al. Exhumation history of the Jiaodong and its adjacent areas since the Late Cretaceous: Constraints from low temperature thermochronology[J]. Science China Earth Sciences, 2017, 60(3): 531−545.

[28] 袁万明, 王世成, 王兰芬. 东昆仑五龙沟金矿床成矿热历史的裂变径迹热年代学证据[J]. 地球学报, 2000, 21(4): 389

−395.
YUAN Wan-ming, WANG Shi-cheng, WANG Lan-fen. Metallogenic thermal history of the Wulonggou gold deposits in east Kunlun mountains in the light of fission track thermochronology[J]. Acta Geoscientia Sinica, 2000, 21(4): 389−395.
[29] 袁万明. 矿床保存变化研究的热年代学技术方法[J]. 岩石学报, 2016, 32(8): 2571−2578.
YUAN Wan-ming. Thermochronological method of revealing conservation and changes of mineral deposits[J]. Acta Petrologica Sinica, 2016, 32(8): 2571−2578.
[30] GROVES D I, CONDIE K C, GOLDFARB R J, et al. Secular changes in global tectonic processes and their influence on the temporal distribution of gold-bearing mineral deposits[J]. Economic Geology, 2005, 100(2): 203−224.
[31] KESLER S E, WILKINSON B H. The role of exhumation in the temporal distribution of ore deposits[J]. Economic Geology, 2006, 101(5): 919−922.
[32] 张丽婷, 袁万明, 李 娜, 等. 甘孜−理塘金成矿带构造活动的磷灰石裂变径迹年代学制约[J]. 岩石学报, 2015, 31(11): 3353−3362.
ZHANG Li-ting, YUAN Wan-ming, LI Na, et al. Apatite fission track constrains on tectonic activities in Ganzi-Litang gold belt, Qinghai-Tibet Plateau[J]. Acta Petrologica Sinica, 2015, 31(11): 3353−3362.
[33] TIAN Peng-fei, YUAN Wan-ming, YANG Xiao-yong, et al. Multi-stage tectonic events of the Eastern Kunlun Mountains, Northern Tibetan Plateau constrained by fission track thermochronology[J]. Journal of Asian Earth Sciences, 2020, 198: 104428.
[34] DENG Jun, WANG Chang-ming, BAGAS Leon, et al. Cretaceous-Cenozoic tectonic history of the Jiaojia Fault and gold mineralization in the Jiaodong Peninsula, China: constraints from zircon U-Pb, illite K-Ar, and apatite fission track thermochronometry[J]. Mineralium Deposita, 2015, 50(8): 987−1006.
[35] WANG Chang-ming, DENG Jun, SANTOSH M, et al. Timing, tectonic implications and genesis of gold mineralization in the Xincheng gold deposit, China: C-H-O isotopes, pyrite Rb-Sr and zircon fission track thermochronometry[J]. Ore Geology Reviews, 2015, 65: 659−673.
[36] LIANG Ya-yun, LIU Xue-fei, QIN Chen, et al. Petrogenesis of Early Cretaceous mafic dikes in southeastern Jiaolai basin, Jiaodong Peninsula, China[J]. International Geology Review, 2017, 59(2): 131−150.
[37] CAI Ya-chun, FAN Hong-rui, SANTOSH M, et al. Decratonic gold mineralization: Evidence from the Shangzhuang gold deposit, eastern North China Craton[J]. Gondwana Research, 2018, 54: 1−22.
[38] WU Lin, MONIE Patrick, WANG Fei, et al. Multi-phase cooling of Early Cretaceous granites on the Jiaodong Peninsula, East China: Evidence from 40Ar/39Ar and (U-Th)/He thermochronology[J]. Journal of Asian Earth Sciences, 2018, 160: 334−347.
[39] ZHANG Liang, YANG Li-qiang, WANG Yu, et al. Thermochronologic constrains on the processes of formation and exhumation of the Xinli orogenic gold deposit, Jiaodong Peninsula, Eastern China[J]. Ore Geology Reviews, 2017, 81: 140−153.
[40] ZHANG Liang, YANG Li-qiang, WEINBERG Roberto F, et al. Anatomy of a world-class epizonal orogenic-gold system: A holistic thermochronological analysis of the Xincheng gold deposit, Jiaodong Peninsula, Eastern China[J]. Gondwana Research, 2019, 70: 50−70.
[41] 赵宝聚, 高明波, 李亚东, 等. 胶莱盆地东北缘龙口−土堆矿区金矿床成矿规律研究[J]. 地质学报, 2019, 93(S1): 1−11.
ZHAO Bao-ju, GAO Ming-bo, LI Ya-dong, et al. Study on metallogenic regularity of gold deposits in Longkou-Tudui mining area on the northeastern margin of Jiaolai basin[J]. Acta Geologica Sinica, 2019, 93(S1): 1−11.
[42] 耿 科, 李大鹏, 胡秉谦, 等. 胶东西涝口金矿深部 110 Ma 角闪辉长岩脉及其对成矿时代的约束[J]. 矿床地质, 2020, 39(6): 974−994.
GENG Ke, LI Da-peng, HU Bing-qian, et al. 110 Ma hornblende gabbro dyke in deep part of Xilaokou gold deposit, Jiaodong and its constraints on metallogenic time[J]. Mineral Deposits, 2020, 39(6): 974−994.
[43] 李洪奎, 时文革, 李逸凡, 等. 山东胶东地区金矿成矿时代研究[J]. 黄金科学技术, 2013, 21(3): 1−9.
LI Hong-kui, SHI Wen-ge, LI Yi-fan, et al. Study on gold mineralization ages in Jiaodong area, Shandong Province[J]. Gold Science and Technology, 2013, 21(3): 1−9.
[44] 宋明春, 林少一, 杨立强, 等. 胶东金矿成矿模式[J]. 矿床地质, 2020, 39(2): 215−236.
SONG Ming-chun, LIN Shao-yi, YANG Li-qiang, et al. Metallogenic model of Jiaodong Peninsula gold deposits[J]. Mineral Deposits, 2020, 39(2): 215−236.
[45] 宋明春, 宋英昕, 丁正江, 等. 胶东金矿床: 基本特征和主要

争议[J]. 黄金科学技术, 2018, 26(4): 406−422.

SONG Ming-chun, SONG Ying-xin, DING Zheng-jiang, et al. Jiaodong gold deposits: Essential characteristics and major controversy[J]. Gold Science and Technology, 2018, 26(4): 406−422.

[46] 宋明春, 宋英昕, 李　杰, 等. 胶东与白垩纪花岗岩有关的金及有色金属矿床成矿系列[J]. 大地构造与成矿学, 2015, 39(5): 828−843.

SONG Ming-chun, SONG Ying-xin, LI Jie, et al. Metallogenic series of gold and nonferrous metal deposits related to Cretaceous granites in eastern Shandong Peninsula, China[J]. Geotectonica et Metallogenia, 2015, 39(5): 828−843.

[47] HURFORD A J, GREEN P F. A users' guide to fission track dating calibration[J]. Earth and Planetary Science Letters, 1982, 59(2): 343−354.

[48] GALBRAITH R F, LASLETT G M. Statistical models for mixed fission track ages[J]. Nuclear Tracks and Radiation Measurements, 1993, 21(4): 459−470.

[49] DONELICK R A. A method of fission-track analysis utilizing bulk chemical etching of apatite: US5267274[P]. 1993-11-30.

[50] BURTNER R L, NIGRINI A, DONELICK R A. Thermochronology of Lower Cretaceous source rocks in the Idaho-Wyoming thrust belt[J]. AAPG Bulletin, 1994, 78(10): 1613−1636.

[51] KETCHAM R A, DONELICK R A, DONELICK M B. AFTSolve: A program for multi-kinetic modeling of apatite fission-track data[J]. Geological Materials Research, 2000, 2(1): 1−32.

[52] KETCHAM R A. Forward and inverse modeling of low-temperature thermochronometry data[J]. Reviews in Mineralogy and Geochemistry, 2005, 58(1): 275−314.

[53] 杨忠虎, 李　楠, 张　良, 等. 西秦岭阳山金矿带成矿热年代学: 锆石和磷灰石裂变径迹研究[J]. 地学前缘, 2019, 26(5): 174−188.

YANG Zhong-hu, LI Nan, ZHANG Liang, et al. Geochronology of mineralization in the Yangshan gold belt, West Qinling: A study on zircon and apatite fission track[J]. Earth Science Frontiers, 2019, 26(5): 174−188.

[54] 韩　伟, 李玉宏, 刘　溪, 等. 鄂尔多斯盆地东南南召地区中生代以来的构造演化研究: 来自低温热年代学的证据[J]. 地质学报, 2020, 94(10): 2834−2843.

HAN Wei, LI Yu-hong, LIU Xi, et al. Tectonic evolution since the Mesozoic of the Nanzhao area in southeast of the Ordos Basin: Evidence from low-temperature thermal chronology[J]. Acta Geologica Sinica, 2020, 94(10): 2834−2843.

[55] 吏成辉, 程银行, 王铁军, 等. 松辽盆地新生代构造演化对砂岩型铀矿成矿的控制作用: 来自磷灰石裂变径迹的证据[J]. 地质学报, 2020, 94(10): 2856−2873.

LI Cheng-hui, CHENG Yin-hang, WANG Tie-jun, et al. The controlling effect of Cenozoic tectonic evolution on the mineralization of sandstone-type uranium deposits in the Songliao Basin: Evidence from apatite fission tracks[J]. Acta Geologica Sinica, 2020, 94(10): 2856−2873.

[56] SHUI Peng. Study on geological characteristics and genetic mechanism of the Guocheng-Liaoshang Gold Deposits in Northeast Margin of the Jiaolai Basin[D]. Beijing: China University of Geosciences(Beijing), 2019.

[57] LIU Xuan, FAN Hong-rui, EVANS Noreen J, et al. Exhumation history of the Sanshandao Au deposit, Jiaodong: Constraints from structural analysis and (U-Th)/He thermochronology[J]. Scientific Reports, 2017, 7(1): 7787.

[58] CANDE S C, LABREQUE J L, LARSON R L, et al. Map of magnetic lineations of the worlds ocean basins (Scale 1:27.4 million at the Equator)[CM]. Tulsa: American Association of Petroleum Geologists, 1989.

[59] ROEDDER E, BELKIN H E. Fluid inclusions in salt from the Rayburn and Vacherie Domes, Louisiana[R]. Geological Survey, Washington, DC (USA), 1979: 79−1675.

[60] ROEDDER E, BODNAR R J. Geologic pressure determinations from fluid inclusion studies[J]. Annual Review of Earth and Planetary Sciences, 1980, 8: 263−301.

[61] SIBSON R H, SCOTT J. Stress/fault controls on the containment and release of overpressured fluids: examples from gold-quartz vein systems in Juneau, Alaska; Victoria, Australia and Otago, New Zealand[J]. Ore Geology Reviews, 1998, 13(1/2/3/4/5): 293−306.

[62] 谢友良, 邵拥军, 冯雨周, 等. 甘肃李坝金矿床流体包裹体特征与矿床成因[J]. 中国有色金属报, 2018, 28(5): 994−1007.

XIE You-liang, SHAO Yong-jun, FENG Yu-zhou, et al. Characteristic of fluid inclusions and genesis of Liba gold deposit, Gansu Province, China[J]. The Chinese Journal of Nonferrous Metals, 2018, 28(5): 994−1007.

Denudation degree and deep prospecting potential of gold deposits in Guocheng-Yazi fault zone, Jiaolai basin

CHEN Yuan-lin[1, 2], LI Huan[1, 2], ZHENG Chao-yang[3], LI Da-dou[4]

(1. School of Geosciences and Info-Physics, Central South University, Changsha 410083, China;
2. Key Laboratory of Metallogenic Prediction of Nonferrous Metals and Geological Environment Monitoring, Central South University, Changsha 410083, China;
3. College of Resources and Environmental Engineering, Guizhou University, Guiyang 550025,China;
4. No.1 Institute of Geology and Mineral Resources of Shandong Province, Jinan 250100, China)

Abstract: The Guocheng-Yazi fault belt in the Jiaolai basin is an important gold metallogenic area discovered in recent years, and a number of large and medium-sized to super-large gold deposits have been discovered continuously. However, n the deep prospecting and exploration work in the ore concentration area has not made a major breakthrough. In this paper, through the systematic collection of ore-forming rock and ore samples, the apatite single mineral was separated. The fission track thermochronology method was used to reveal the temperature-time evolution of the ore body in the study area. We inversed the thermal evolution history of the rock mass and ore body, analyzed the structural transformation of the deposit after mineralization, quantitatively calculated the uplift denudation rate of the rock mass and ore body, and summarized the denudation and preservation law of the deposit. The results show that the Guocheng-Yazi fault zone gold concentration area mainly experienced two stages of post-mineralization thermal history of 110−20 Ma and 20−0 Ma, and the two-stage uneven uplift and cooling process was affected by the multi-stage proliferation and expansion process of the Pacific Ocean. Based on the analysis of the thermal history evolution of apatite fission track, combined with the regional paleogeothermal gradient, metallogenic depth and the thickness of Jurassic and Cretaceous continental sedimentary strata, the total erosion depth of the strata in the study area from Cretaceous to now is calculated to be about 5.33 km, and the metallogenic depth of the ore body in the gold belt is 5.62 km, indicating that the ore body in the Guocheng-Yazi fault zone has been subjected to a large degree of uplift and denudation. It is speculated that the part of the fault zone with less erosion of the southwest strata has great prospecting potential, and the deep gold ore body positioning model of the Guocheng-Yazi fault zone is established to evaluate the deep prospecting potential.

Key words: Queshan pluton; Muniushan pluton; thermal history simulation; uplift-denudation; deep exploration; metallogenic depths

Foundation item: Project(2016YFC0600104) supported by the National Key Research and Development Program of China; Project(XY-DZ2020081) supported by the Geological Research Project of Xintai Gold Mining Co., Ltd. (Yantai, Shandong, China) of China National Gold Group Co., Ltd.

Received date: 2021-07-15; **Accepted date:** 2021-10-08

Corresponding author: LI Huan; Tel: +86-18827415616; E-mail: lihuan@csu.edu.cn

(编辑　何学锋)